Photoswitches

Heterocyclic Hemithioindigos: Highly Advantageous Properties as Molecular Photoswitches**

Verena Josef, Frank Hampel, and Henry Dube*

Abstract: A survey of heterocyclic hemithioindigo photoswitches is presented identifying a number of structural motives with outstanding property profiles. The highly sought-after combination of pronounced color change, quantitative switching in both directions, exceptional high quantum yields, and tunable high thermal stability of metastable states can be realized with 4-imidazole, 2-pyrrole, and 3-indole-based derivatives. In the former, an unusual preorganization using isomer selective chalcogen- and hydrogen bonding allows to precisely control geometry changes and tautomerism upon switching. Heterocyclic hemithioindigos thus represent highly promising photoswitches with advanced capabilities that will be of great value to anyone interested in establishing defined and reversible control at the molecular level.

Molecular photoswitches are prominent molecular tools to control processes at the nanoscale by light irradiation.[1] They are used in a broad spectrum of applications ranging from molecular machine building[2] and supramolecular chemistry[3] to catalysis,[4] chemical biology,[5] materials sciences,[6] or 3D printing technology,[7] to name just a few. For each application the properties of photoswitches need to be tailored to harness their functionalities with highest effectiveness. Much present research is therefore devoted to consciously tailoring properties of existing photoswitching motives or developing new photoswitch architectures entirely.[8] When it comes to the properties of photoswitches the enrichment of a particular isomer in the photostationary state (pss, depending on the wavelength of irradiation) and the efficiency of the light-induced switching process (quantum yield) are standing out. Visible light addressability, high thermal stability of isomeric states and precision geometry

control are further crucial properties that need to be present for optimal performance. Only few photoswitches allow to quantitatively transform the bulk isomer population reversibly from one state to the other, fewer so at a very quick pace.[9] Key to this desired behavior is the favorable combination of large absorption band separation between isomers and high quantum yields. Even less performance is seen when further preferred properties as mentioned above are added to the list and thus new photoswitches and concepts are urgently needed to alleviate this situation.

Hemithioindigo (HTI) chromophores[10] belong to the emerging class of indigoid photoswitches[10,11] and have gained considerable traction in the recent years as a versatile photoswitch motive. They possess a number of advantageous properties such as visible light responsiveness, considerable absorption differences between isomers, rigid and thus predictable structures, high thermal stability of metastable states, and straight forward synthetic access.[12] Mechanistic studies have already revealed a large influence of substitution on the photophysical and photochemical properties and allow to tune them much more consciously.[13] Consequentially HTIs have found their way into many different applications already, including molecular machines,[14] supramolecular chemistry,[15] chemical biology,[16] or multi-switches,[17] photosalient behavior,[18] and molecular logic.[19] The unsubstituted core chromophore of HTI allows almost quantitative isomer enrichment in the pss at suitable wavelengths of irradiation (94 % *E* isomer at 420 nm and 100 % *Z* isomer at 505 nm, respectively) but substitutions can lead to diminished yield of the *E* isomer upon irradiation.[13c,20] This problem has been addressed by *Newhouse* and co-workers using pyrrole and 2-imidazole substituted HTIs, which leads to improved and nearly quantitative *E* or *Z* isomer enrichment in the pss at suitable wavelengths.[21] The beneficiary effect of the pyrrole is thought to be manifested via its hydrogen bonding capacity especially to the carbonyl function in the *E* isomeric state. A similar hydrogen bonding interaction with pyrrole has been explored earlier in the related hemiindigo photoswitches by *Arai and Ikegami*.[22] The possible advantageous effects of heterocyclic derivatization of photoswitches are however not limited to indigoid chromophores as recent work on azobenzene[23] or earlier work on diarylethenes[24] have shown. A variety of weak interactions are coming into play when heterocycles are introduced into photoswitches oftentimes leading to significant improvements of the switching, new levels of control, and unusual effects on geometries or electronics. In this work we broadly explore the effects of heterocycle derivatization of HTI and show how especially

[*] V. Josef, F. Hampel, H. Dube
Friedrich-Alexander Universität Erlangen-Nürnberg, Department of Chemistry and Pharmacy
Nikolaus-Fiebiger-Str. 10, 91058 Erlangen (Germany)
E-mail: henry.dube@fau.de

Angew. Chem. Int. Ed. **2022,** *61,* e202210855 (1 of 8)

© 2022 The Authors. Angewandte Chemie International Edition published by Wiley-VCH GmbH

4-imidazole and 3-indole substitution allow to achieve outstanding photoswitching performances with visible light irradiation. The imidazole substituent shows a highly interesting change of hydrogen bonding pattern, where the two different tautomers are reversibly interchanged upon switching. This effect is the result of a competing hydrogen versus chalcogen bonding[25] interaction, which offers unique opportunities as preorganization tool in HTI photoswitch architectures.

To scrutinize the effect of heterocyclic substitution on HTI photoswitch performance 16 different motives were incorporated such as imidazole, indole, pyridine, quinoline, thiazole, pyrrole (for comparison purposes as pyrrole-HTI compounds have been described already[21,26]), pyrazole, benzofuran, and benzothiophene. This selection covers electron rich and electron poor heterocycles with and without hydrogen bonding capacity, different connection positions and also additional halogen substitutions enabling late-stage diversification. The set includes eminent hetero-

cycle motives prevalent in pharmaceutical and medicinal chemistry (e.g. indoles, pyridines, imidazole, or quinoline) and also complements known structures such as pyrrole, furan, thiophene[21] or pyridine[27] derivatives of HTI with the corresponding benzene-annulated analogues (indoles, benzofuran, benzothiophene, and quinoline). Motives that show significant effects in azobenzene photoswitches have also been included such as thiazole or pyrazole. We have refrained from introducing significant steric hindrance however, in order to observe the unperturbed heterocycle properties especially with respect to electronic effects. The corresponding Het-HTIs **1–16** are depicted in Figure 1.

Synthesis of Het-HTIs follows established protocols for HTI synthesis[11a,13c] and encompasses the condensation reaction between benzothiophenone and the respective heterocyclic aldehyde as key step (for details see the Supporting Information). Crystals suitable for X-ray diffraction analysis were obtained for Het-HTIs *Z*-**1**, *Z*-**4**, *E*-**8**, and
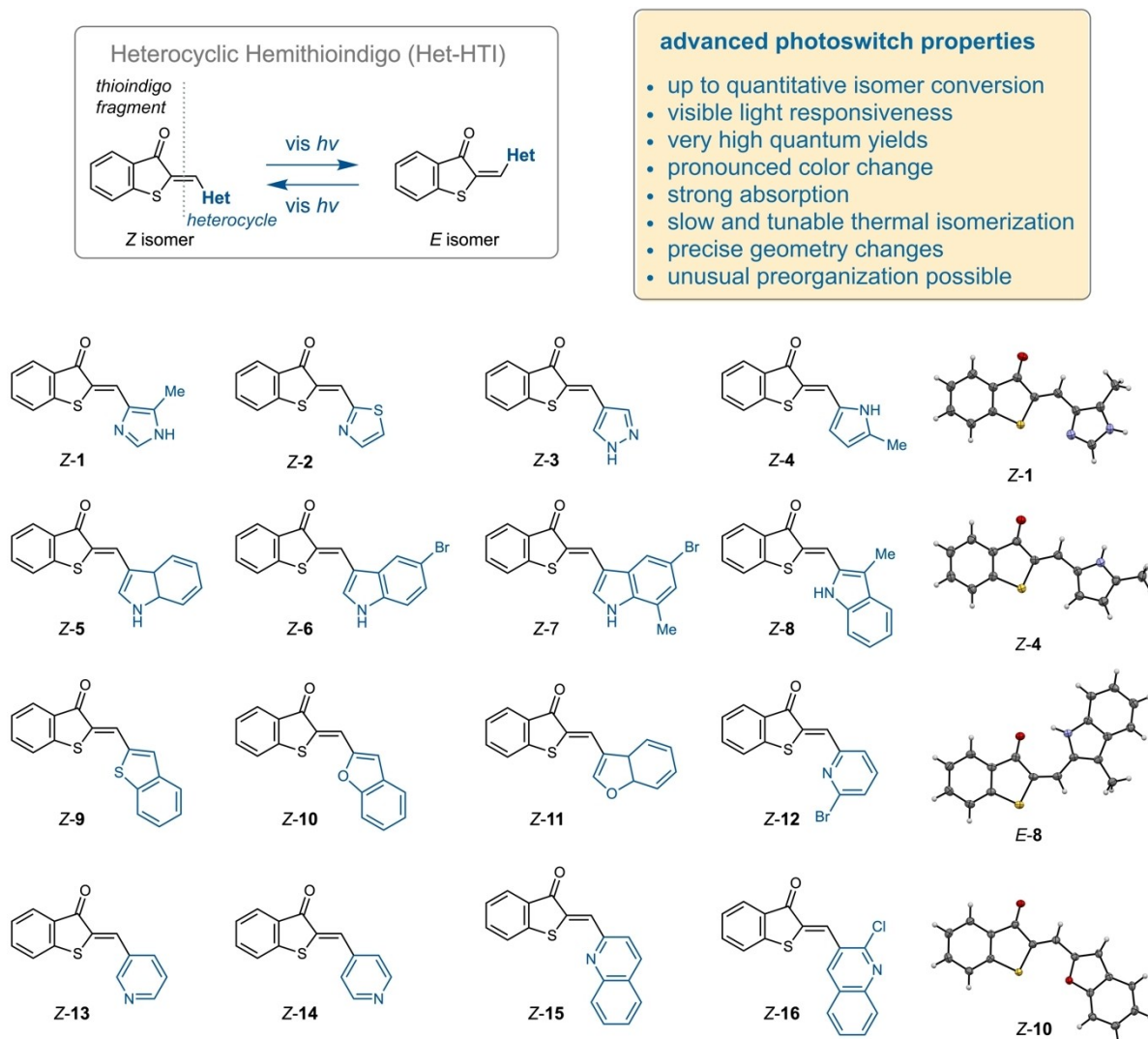

Figure 1. Heterocyclic HTI photoswitches undergo visible light responsive double bond isomerization. Depiction of Het-HTIs **1–16** investigated in this study and the corresponding structures in the crystalline state of Het-HTIs *Z*-**1**, *Z*-**4**, *E*-**8**, and *Z*-**10**.

Z-**10** and the corresponding molecular structures in the crystalline state[28] are depicted in Figure 1 as well.

The (photo)-physical and photochemical properties of Het-HTIs **1**–**16** were scrutinized in different solvents to elucidate additional solvent effects and test the robustness of the properties and switching performances. First the thermal behavior was analyzed (for details see the Supporting Information, Figure S44 to S58). For almost all investigated Het-HTIs the *Z* isomers are the thermodynamically most stable states, which renders the corresponding *E* isomers metastable. For this reason, leaving *E* isomer enriched solutions in the dark at elevated temperatures leads to thermal back-isomerization to the more stable *Z* isomers. Different to the parent HTI, thermal isomerization to the *Z* isomers is not always quantitative and in some cases a thermal equilibrium with both *Z* and *E* isomers being present is established. Kinetic analysis delivers the corresponding Gibbs energies of activation $\Delta G^{\ddagger}$, which range between 20.0 kcal mol^{-1} and 30.5 kcal mol^{-1}. The influence of the solvent is typically significant and an increase in polarity leads to increased rate of thermal isomerization. This is most clearly seen in the pyrrole derivative **4** with $\Delta G^{\ddagger} =$ 30.5 kcal mol^{-1} in toluene-d_8 and $\Delta G^{\ddagger} = 21.1$ kcal mol^{-1} in DMSO solution. With such pronounced differences in $\Delta G^{\ddagger}$

the corresponding half-lives of the metastable *E* isomers can be tuned consciously by many orders of magnitude depending on the particular heterocycle and solvent that is used. With the lower limit of $\Delta G^{\ddagger} = 20.0$ kcal mol^{-1} still sizeable life-times of the metastable isomers of Het-HTIs in the minute range at ambient temperatures are established. The only exception is Het-HTI **8**, for which the *E* isomer is stable in solution, most probably because of pronounced and favorable intramolecular hydrogen bonding to the carbonyl group. The latter is clearly evidenced in the crystalline structure as shown in Figure 1.

The photophysical and photochemical properties of Het-HTIs **1**–**16** were investigated next and the corresponding quantified behavior is summarized in Table 1. Molar extinction coefficients in different solvents were measured to establish photochromism and wavelength selective photoswitching. Strong absorptions are observed in all cases within the visible region of the electromagnetic spectrum. Absorption changes between isomers are pronounced for almost all derivatives and maxima differences up to 50 nm are found. The maximum extinction coefficients are typically in the range of 15000 L mol^{-1} cm^{-1} but for the indole derivatives they reach up to 44000 L mol^{-1} cm^{-1} rendering the latter into very good chromophores (all extinction

Table 1: Summary of (photo)physical properties of Het-HTIs **1** to **16**.

Compound	Solvent	Isomer yield in pss (at irr. λ in nm)	Quantum yield Φ ($Z{\rightarrow}E$, $E{\rightarrow}Z$)	Thermal isomerization $\Delta G^{\ddagger}$ in kcal mol^{-1}	*E* isomer half lives linearly extrapol. to 25 °C	Extinction λ_{max} in nm (isomer, ε in L mol^{-1} cm^{-1})
1	C$_6$H$_6$	100% *E* (420), 100% *Z* (515)		27.7	82 d	450 (*Z*, 13 000), 497 (*E*, 14 000)
	THF	91% *E* (430), 100% *Z* (530)	69%, 43%			452 (*Z*, 32 900), 492 (*E*, 27 100)
	ACN	93% *E* (405), 100% *Z* (530)	43%, 17%	24.2	12 h	448 (*Z*, 17 400), 488 (*E*, 18 800)
	MeOH	81% *E* (450), 85% *Z* (505)		20.0	1 min	
2	DMSO	–				455 (*Z*, 27 800), 609 (*Z*, 900)
3	toluene	84% *E* (405), 100% *Z* (505)	34%, 17%	24.0	12 h	427 (*Z*, 15 500), 450 (*E*, 10 600)
	DMSO	76% *E* (405), 97% *Z* (505)		21.0	5 min	433 (*Z*, 23 400), 448 (*E*, 15 500)
4	toluene	100% *E* (420), 94% *Z* (505)		30.5	35 years	468 (*Z*, 12 400), 519 (*E*, 15 700)
	THF	95% *E* (450), 95% *Z* (530)	65%, 41%			471 (*Z*, 41 000), 516 (*E*, 33 800)
	DMSO	87% *E* (420), 95% *Z* (590)	36%, 43%	21.1	5 min	481 (*Z*, 17 000), 521 (*E*, 19 100)
5	THF	89% *E* (405), 92% *Z* (530)	35%, 26%	20.4	1 min	455 (*Z*, 41 900), 487 (*E*, 38 900)
6	THF	87% *E* (405), 100% *Z* (530)	42%, 54%	22.6	25 min	452 (*Z*, 44 000), 483 (*E*, 44 000)
7	THF	85% *E* (405), 100% *Z* (530)	39%, 48%	22.4	25 min	454 (*Z*, 44 500), 485 (*E*, 42 000)
8						532 (*E*, 33 100)
9	toluene	95% *E* (450), 88% *Z* (530)	53%	26.5	15 d	445 (*Z*, 32 000), 475 (*E*, 23 900)
	DMSO	80% *E* (405), 46% *Z* (505)		21.1	5 min	
10	toluene					461 (*Z*, 35 100), 482 (*E*, 31 800)
	ACN	80% *E* (405), 46% *Z* (505)	19%, 8%	25.5 (DMSO)	3 d	456 (*Z*, 40 000), 477 (*E*, 35 000)
11	toluene			24.3 (DMSO)	12 h	432 (*Z*, 17 200), 456 (*E*, 16 000)
12	C$_6$H$_6$	decomposition				
	DMSO	decomposition				434 (*Z*, 10 300)
13	C$_6$H$_6$	decomposition				
	DMSO	decomposition				433 (*Z*, 9 500)
	ACN	70% *E* (450) decomposition				
14	C$_6$H$_6$	decomposition				
	DMSO	decomposition				451 (*Z*, 17 000)
15	toluene	decomposition				
	DMSO	decomposition				459 (*Z*, 17 800)
16	toluene	decomposition				
	DMSO	decomposition				446 (*Z*, 9 100)

coefficients are given in the Supporting Information). Irradiation with light of different wavelengths was then conducted until no further changes in isomer composition were observed in the pss. For this purpose, UV/Vis as well as ^{1}H NMR spectroscopy allowed to quantify the switching. Again, clear trends were observed for the various heterocyclic structures. In the case of electron poor heterocycles, i.e. thiazole (Het-HTI **2**), pyridines (Het-HTI **12** and Het-HTI **14**), or quinolines (Het-HTIs **15** and **16**) the absorption changes between isomers and thus photochromism are strongly diminished. No favorable and reversible photoswitching is observed for these derivatives. Only if the electron-withdrawing effect on the photoisomerizable double bond is suppressed like in 3-pyridine derivative Het-HTI **13**, absorption changes between isomers are increased but reversible switching is still hampered by significant photodestruction (see Figure S37 in the Supporting Information). Similar compromised photostability has been reported for pyridinium-HTIs in a recent publication[27] however, more proper switching for ethyl-substituted variants have been described earlier.[15c] If electron-rich heterocycles such as pyrrole or 3-indoles are used (Het-HTI **4** and Het-HTI **5** to **7**) absorption band separation is pronounced with up to 50 nm shifts between λ_{max} values of the two isomers (Figure 2, for further details see the Supporting Information and

Figure S2 to S19). In these cases, reversible photoswitching is highly favorable and very strong isomer accumulation under irradiation is possible in both directions (Supporting Information, Table S1 to S9). This behavior is somewhat comparable to earlier studies on strongly donor substituted HTIs.[13c, d] The 2-indole derivative Het-HTI **8** shows a very different behavior with the thermodynamically stable *E*-isomer being predominant in solution. The switching capacity is strongly diminished despite its close structural relation to the pyrrole derivative Het-HTI **4**. This substitution-position effect highlights the importance of electron donation over hydrogen bonding capacity in the indole derivatives. It also shows that intramolecular hydrogen bonding can lead to abolished photoswitching capacity when structural stabilization of one particular isomer (*E* in this case) is too pronounced.

A very interesting derivative is represented by 4-imidazole substituted Het-HTI **1** (see e.g. Figure 2). In this case large absorption band separation between the isomers and high photoisomerization efficiency lead to the highly sought after, yet rarely observed, quantitative *Z* to *E* and *E* to *Z* photoswitching. For this purpose, blue and green light can be used and the switching properties are not strongly affected by polarity of the solvent. Even in very polar acetonitrile photoisomerization in both directions is almost
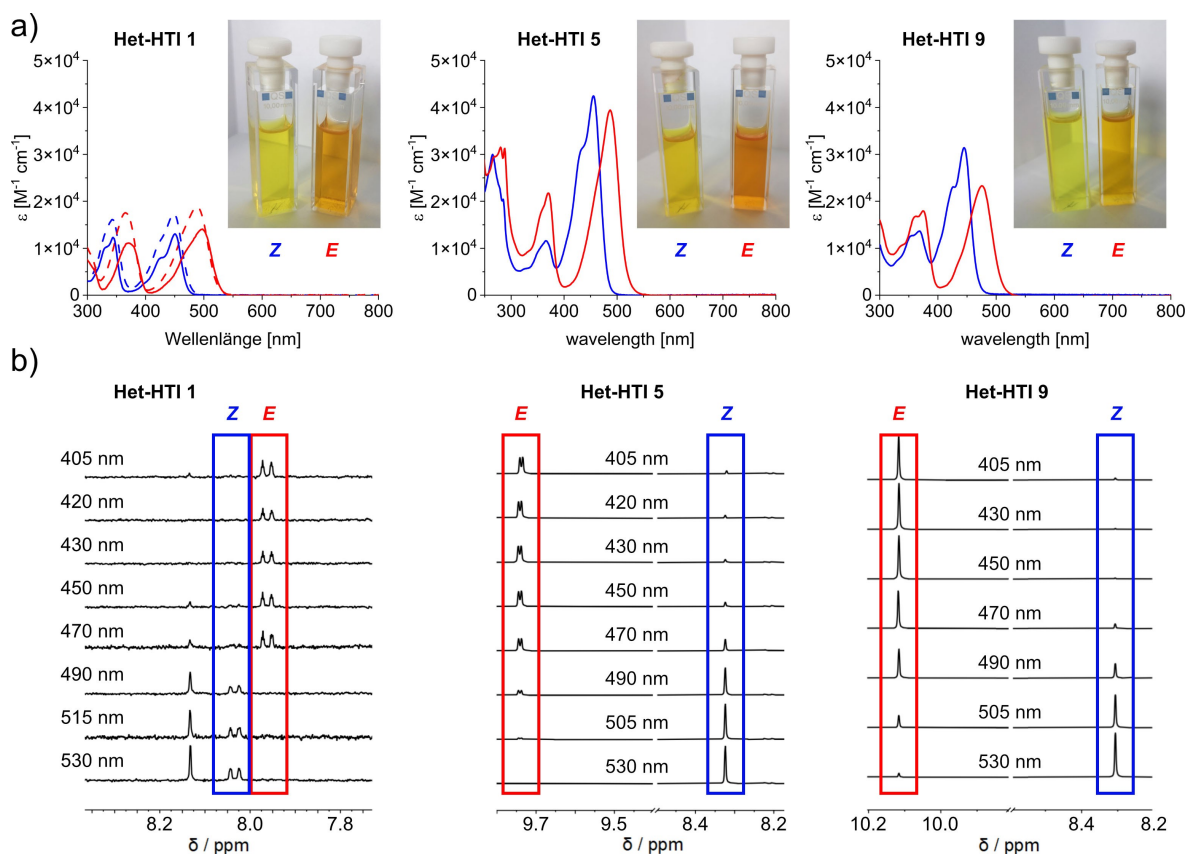

Figure 2. Absorption and photoswitching behavior of selected Het-HTIs **1**, **5**, and **9**. a) Molar extinction coefficients. Photographs show cuvettes containing the respective toluene solutions after irradiation to the pss with green (left) and blue light (right). b) Quantified photoswitching of Het-HTIs using ^{1}H NMR spectroscopy (from left to right; Het-HTI **1** (1.95 mM, benzene-d_6), Het-HTI **5** (4.05 mM, THF-d_8), Het-HTI **9** (3.85 mM, toluene-d_8). Spectra were recorded after reaching the pss at the indicated wavelengths of irradiation.

quantitative (93 % *E* isomer accumulation and 100 % *Z* isomer accumulation). Only in MeOH solution is *E* isomer enrichment diminished to 80 %. Thermal stability of Het-HTI **1** can be tuned to allow for minutes to months persistence of the metastable *E* isomer at ambient temperatures in solution.

When assessing the exact geometry changes upon switching (see the structure analysis section of the Supporting Information for full details) Het-HTI **1** shows a very noteworthy behavior. In principle there are two different tautomers as well as two different rotamers possible for the imidazole in each the *Z* as well as *E* isomeric state, which leads to eight possible structures overall and different associated methyl-group orientations with respect to the thioindigo fragment. In solution as well as the crystalline state however, a clear preference for only one such structure is observed for each configuration of the double bond, which evidences a strong preorganization for Het-HTI **1** (Figure 3 a and b). The preorganization is however quite unusual. In the *Z* isomer the imidazole tautomer harbors the NH proton next to the methyl group in a rotamer that is turned away from the sulfur atom. This orientation establishes a close chalcogen-bonding contact between the imine-like nitrogen of the imidazole and the sulfur atom with a corresponding

short distance of 2.92 Å (as measured in the crystal, see Figure 3b). This preferred isomer is also evidenced in solution by NMR spectroscopy (see Figure 3c and d and the Supporting Information for further details). In the *E* isomer however, the tautomer as well as rotamer state change and now the NH proton is residing at the other nitrogen atom forming an intramolecular hydrogen bond to the carbonyl group of the thioindigo fragment (see the Supporting Information for details). Overall, the intricate balance between avoiding steric clash of the imidazole-methyl group and the thioindigo fragment, tautomerization, as well as chalcogen- and hydrogen-bonding leads to a precisely controlled geometry change in Het-HTI **1**. This is manifested most clearly when following the positional changes of the imidazole-methyl group with respect to the thioindigo fragment during switching (see Figure 3a). A similar chalcogen bonding interaction is also seen in the crystal structure of Het-HTI **10** with the oxygen of the benzofuran oriented towards the sulfur atom at a short distance of 2.90 Å (Figure 1). A similar hydrogen bonding interaction in the *E* isomer is correspondingly seen in the crystal structure of *E*-**8** (Figure 1).

Quantum yield (Φ) measurements (see Supporting Information Figures S59–S83 and Table S10 for details)
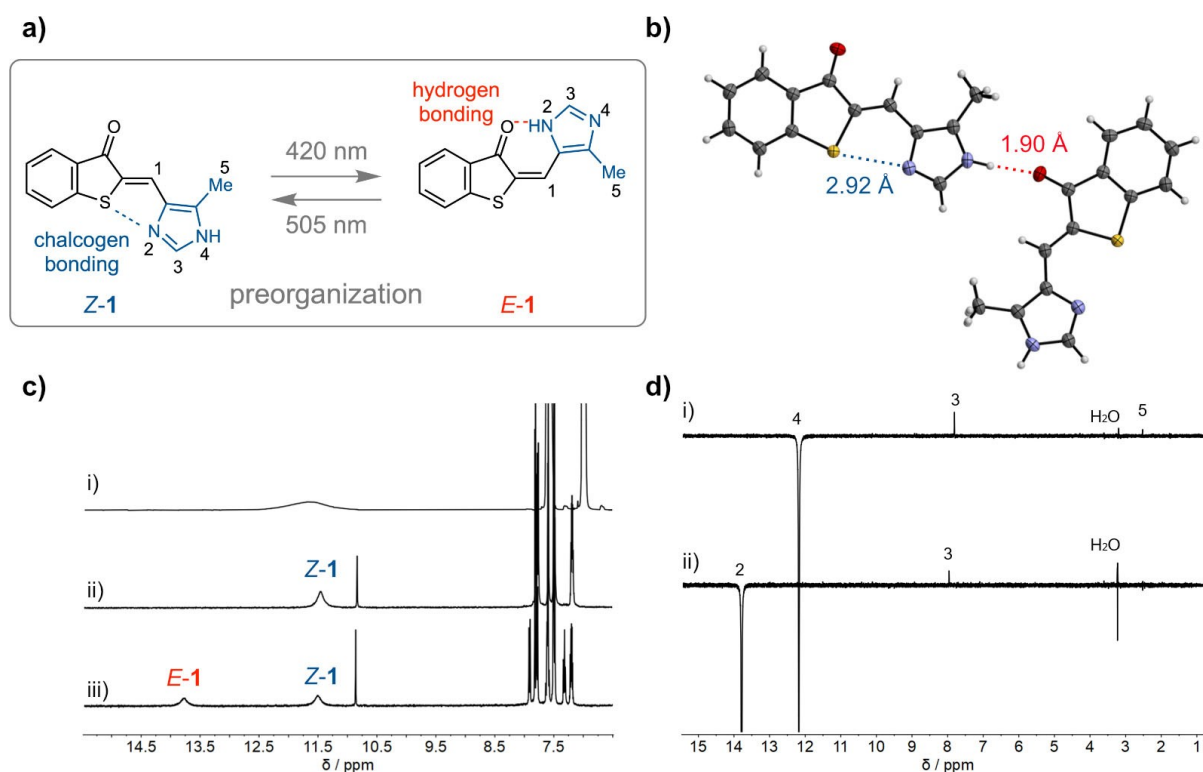

Figure 3. Precise geometry control in Het-HTI **1**. a) Selective chalcogen bonding (blue dotted line) occurs in the *Z*-isomer and selective hydrogen bonding (red dotted line) in the *E*-isomer. Concomitantly a tautomerization is taking place, which positions the acidic NH proton at different nitrogen atoms of the five membered imidazole ring. b) Evidence of the chalcogen bonding in the crystalline state of *Z*-**1**, intermolecular hydrogen bonding locks the NH proton at N4. c) Evidence of the *Z*-**1** isomer structure in solution by NMR spectroscopy using chemical shift analysis in THF-d_8. i) ^{1}H NMR spectrum of imidazole showing the chemical shift of the NH proton as broad signal. ii) ^{1}H NMR spectrum of *Z*-**1** with a similar shifted NH signal. iii) ^{1}H NMR spectrum of a mixture of *Z*-**1** and *E*-**1**, for the latter the NH signal is significantly shifted downfield because of intramolecular hydrogen bonding. d) ROE NMR spectra of *Z*-**1** in THF-d_8 at −80 °C evidencing the position of the NH proton (signal 4) between protons 3 and 5 and thus the tautomeric and rotameric state of *Z*-**1**.

revealed that Het-HTI derivatives are exceptional performers for HTI photoswitches in general. Typically, quantum yields for the photoisomerizations are in the 5%–20% region for HTIs and values for the Z to E direction are significantly higher than for the E to Z direction. However, in special circumstances quantum yields can be increased significantly. For example, twisted and strong donor-bearing HTIs photoisomerize from the Z to the E isomer with up to $\Phi = 56\%$ but only in very apolar solvents such as hexanes.[13d,e] Strong donation in conjugation with the photoisomerizable double bond allows to increase the quantum yields of the E to Z direction and similar values of around $\Phi = 20\%$–30% as for the Z to E direction can be achieved.[13c] However, this increase in photoisomerization efficiency comes at the expense of significantly diminished thermal stability of the metastable states.[13c,19]

Heterocyclic derivatives Het-HTI 1, 4, 6, and 7 are distinct in their behavior as they deliver exceptionally high quantum yields in the range of 39%–69% for both switching directions even in polar solvents (see also Table S10 in the Supporting Information) and while also showing considerable thermal stability of the metastable isomers. Again Het-HTI 1 stands out as best performer with the highest quantum yields of 69% for the Z to E and 43% for the E to Z photoisomerization, closely followed by Het-HTI 4 with similarly high values. To the best of our knowledge such high quantum yields have not been achieved in the entire class of HTI photoswitches. They also compare very well with the top-performing photoswitches of other classes such as azobenzenes[9b,29] or the highly optimized natural counterpart of retinal.[30] It has to be stressed at this point that obtaining very high quantum yields for a full 180° rotation during photoisomerization is not a trivial task and therefore seldomly achieved. The heterocyclic derivatives reported here meet this challenge and in addition to the most efficient photoswitches 1, 4, 6, and 7, Het-HTIs based on pyrazole and unsubstituted 3-indole (Het-HTI 3 and 5 respectively) also possess good to very good quantum yields for both switching directions. Finally, photofatigue was tested for Het-HTIs 1, 5, and 9. After 15 cycles no photodegradation was visible showing very good stability against bleaching for these derivatives (Supporting Information Figure S4, S10, and S15).

General trends can be drawn from comparing the photochemical behavior of Het-HTIs 1–16. Four aspects need to be discussed in this regard, steric and electronic effects, intramolecular interactions, and solvent polarity. Steric effects cannot be compared well in the series because no systematic steric alterations are probed by deliberate substitution without strongly changing electronics and intramolecular interactions such as hydrogen bonding. However, sterics do not appear to play a major role in influencing properties in the series, because all derivatives can adopt a fully planar geometry in both isomeric forms, which allows electronic effects to take full effect (compare for example the similar behavior of 15 and 16). Electronic effects are clearly dominating in the series and in general the more electron rich a heterocycle (as can be determined by e.g. the corresponding Hammett parameters[31]) the better the photoswitching properties. This is most dramatically seen by comparing the favorable photochromic properties of electron rich five-membered heterocycles like 1, 4, 5–7, 9, or 10 with the seriously impeded performance of electron poor six-membered heterocycles 12–16 (poor absorption band separation between isomers, photodegradation irrespective of the position of the heteroatom in the ring). But also within more strongly related structural frameworks, like annulated five-membered heterocycles, the beneficiary effects of electronic donation can clearly be observed. Thus, indole derivatives 5–7 or 8 show larger absorption band separation between Z and E isomers, larger redshift of the absorptions, higher isomer enrichments in the pss, and higher quantum yields as compared to the corresponding benzothiophene and benzofuran derivatives 9, 10, and 11, respectively. This trend is not entirely linear however, as the less electron rich benzothiophene 9 gives overall better performance than the benzofuran-derivatives 10 and 11. The only drawback of 9 is its significantly reduced quantum yield for the E to Z photoisomerization. This behavior is mirrored when comparing pyrrole, furan, and thiophene versions of Het-HTI.[21] Within the series of five-membered heterocycles 1–4 a similar trend is clearly seen, when the electron donating character of the nitrogen heteroatom in 4 (very good performance) is altered into an electron accepting character in 2 (very small absorption differences between isomers, no photoswitching). However, clear trends are not observable when introducing additional (electron withdrawing) nitrogen atoms to the pyrrole core structure (compare 4 with 1 or 3). A noticeable hypsochromic absorption shift is observed by the additional nitrogen heteroatom but photoswitching is generally very favorable for these structures. Solvent polarity does not play a major role with respect to the photoswitching properties, but somewhat diminished isomer enrichment in the pss and decreased quantum yields are observed with increasing polarity. The major effect is on the thermal double bond isomerization as discussed above. Intramolecular hydrogen bonding plays a dual role in the series studied here and is intramolecularly significant only in the E isomeric structures, which are stabilized by this interaction and slowed down in their thermal E to Z isomerization (Het-HTI 1, 4 and 8). When it is forced however, like in Het-HTI 8, the E isomer is too stabilized and switching is abolished. Other weak intramolecular interactions like chalcogen bonding plays a major role in conformation control in the Z isomers as can be seen most pronounced for Het-HTI 1 but also for 10 to some degree. It does not however facilitate switching as Het-HTIs 2, 12, or 15 do no become capable photoswitches despite the opportunity to form chalcogen bonding.

In conclusion, we have probed the photoswitching performance of different heterocyclic HTIs and were able to identify a number of exceptionally performing derivatives. 4-imidazole, 3-indole and 2-pyrrol-based HTIs stand out as most promising core structures for a new generation of ideal photoswitches. They bring forward a suite of highly advantageous properties: strong absorptions and large λ_{max} separation between isomers, quantitative bulk switching, very high quantum yields, and high—yet tunable—thermal stability of

the metastable states. The 4-imidazole derivative Het-HTI **1** represents an exceptional performer and introduces a new concept of preorganization using the intricate balance between chalcogen and hydrogen-bonding to control very precise geometry changes upon switching. Additionally, synthesis of Het-HTIs is straight forward and proceeds in just two steps from commercially available materials. A trend analysis also allows to draw important design principles for maximum photoswitch performance of Het-HTIs. Most important is a strong electron donating character of the heterocycle and thus, five-membered pyrrole- or indole-based motives are most effective. Further property amplification can be done by strategic placement of a second nitrogen heteroatom and hydrogen bonding capacity, which allows more specific control over conformations, isomer stabilities, isomer enrichment in the pss, and elevation of quantum yields. With this survey we have thus identified a number of very promising, high-performance photoswitch motives with unique geometry control as well as design principles for this structure class that will be of great interest to anyone interested in establishing visible light responsiveness at the molecular scale.

Conflict of Interest

The authors declare no conflict of interest.

Data Availability Statement

The data that support the findings of this study are available from the corresponding author upon reasonable request.

[1] a) *Molecular Photoswitches. Chemistry, Properties, and Applications*, Wiley-VCH, Weinheim, **2022**; b) *Molecular Switches, Vol. 1*, Wiley-VCH, Weinheim, **2011**.

[2] a) S. Kassem, T. van Leeuwen, A. S. Lubbe, M. R. Wilson, B. L. Feringa, D. A. Leigh, *Chem. Soc. Rev.* **2017**, *46*, 2592–2621; b) S. Erbas-Cakmak, D. A. Leigh, C. T. McTernan, A. L. Nussbaumer, *Chem. Rev.* **2015**, *115*, 10081–10206; c) V. Balzani, A. Credi, M. Venturi, *Molecular Devices and Machines–Concepts and Perspectives for the Nanoworld*, Wiley-VCH, Weinheim, **2008**.

[3] X. Yao, T. Li, J. Wang, X. Ma, H. Tian, *Adv. Opt. Mater.* **2016**, *4*, 1322–1349.

[4] a) R. Göstl, A. Senf, S. Hecht, *Chem. Soc. Rev.* **2014**, *43*, 1982–1996; b) R. Dorel, B. L. Feringa, *Chem. Commun.* **2019**, *55*, 6477–6486.

[5] a) J. Morstein, D. Trauner, *Curr. Opin. Chem. Biol.* **2019**, *50*, 145–151; b) K. Hüll, J. Morstein, D. Trauner, *Chem. Rev.* **2018**, *118*, 10710–10747; c) W. A. Velema, W. Szymanski, B. L. Feringa, *J. Am. Chem. Soc.* **2014**, *136*, 2178–2191.

[6] a) W. Danowski, T. van Leeuwen, W. R. Browne, B. L. Feringa, *Nanoscale Adv.* **2021**, *3*, 24–40; b) A. Goulet-Hanssens, F. Eisenreich, S. Hecht, *Adv. Mater.* **2020**, *32*, 1905966; c) Z. L. Pianowski, *Chem. Eur. J.* **2019**, *25*, 5128–5144; d) M. Irie, T. Fukaminato, K. Matsuda, S. Kobatake, *Chem. Rev.* **2014**, *114*, 12174–12277.

[7] a) M. Regehly, Y. Garmshausen, M. Reuter, N. F. Konig, E. Israel, D. P. Kelly, C. Y. Chou, K. Koch, B. Asfari, S. Hecht, *Nature* **2020**, *588*, 620–624; b) P. Mueller, M. M. Zieger, B. Richter, A. S. Quick, J. Fischer, J. B. Mueller, L. Zhou, G. U. Nienhaus, M. Bastmeyer, C. Barner-Kowollik, M. Wegener, *ACS Nano* **2017**, *11*, 6396–6403; c) C. A. Spiegel, M. Hippler, A. Münchinger, M. Bastmeyer, C. Barner-Kowollik, M. Wegener, E. Blasco, *Adv. Funct. Mater.* **2020**, *30*, 1907615.

[8] a) J. D. Harris, M. J. Moran, I. Aprahamian, *Proc. Natl. Acad. Sci. USA* **2018**, *115*, 9414–9422; b) D. Bléger, S. Hecht, *Angew. Chem. Int. Ed.* **2015**, *54*, 11338–11349; *Angew. Chem.* **2015**, *127*, 11494–11506.

[9] a) R. Siewertsen, H. Neumann, B. Buchheim-Stehn, R. Herges, C. Näther, F. Renth, F. Temps, *J. Am. Chem. Soc.* **2009**, *131*, 15594–15595; b) W. Moormann, T. Tellkamp, E. Stadler, F. Rohricht, C. Nather, R. Puttreddy, K. Rissanen, G. Gescheidt, R. Herges, *Angew. Chem. Int. Ed.* **2020**, *59*, 15081–15086; *Angew. Chem.* **2020**, *132*, 15193–15198; c) S. Fukumoto, T. Nakashima, T. Kawai, *Angew. Chem. Int. Ed.* **2011**, *50*, 1565–1568; *Angew. Chem.* **2011**, *123*, 1603–1606.

[10] S. Wiedbrauk, H. Dube, *Tetrahedron Lett.* **2015**, *56*, 4266–4274.

[11] a) C. Petermayer, H. Dube, *Acc. Chem. Res.* **2018**, *51*, 1153–1163; b) S. Thumser, L. Köttner, N. Hoffmann, P. Mayer, H. Dube, *J. Am. Chem. Soc.* **2021**, *143*, 18251–18260.

[12] a) J. I. Lee, *Bull. Korean Chem. Soc.* **2021**, *42*, 1210–1219; b) M. T. Konieczny, W. Konieczny, *Heterocycles* **2005**, *65*, 451–464.

[13] a) A. Nenov, T. Cordes, T. T. Herzog, W. Zinth, R. de Vivie-Riedle, *J. Phys. Chem. A* **2010**, *114*, 13016–13030; b) J. Plötner, A. Dreuw, *J. Phys. Chem. A* **2009**, *113*, 11882–11887; c) B. Maerz, S. Wiedbrauk, S. Oesterling, E. Samoylova, A. Nenov, P. Mayer, R. de Vivie-Riedle, W. Zinth, H. Dube, *Chem. Eur. J.* **2014**, *20*, 13984–13992; d) S. Wiedbrauk, B. Maerz, E. Samoylova, A. Reiner, F. Trommer, P. Mayer, W. Zinth, H. Dube, *J. Am. Chem. Soc.* **2016**, *138*, 12219–12227; e) S. Wiedbrauk, B. Maerz, E. Samoylova, P. Mayer, W. Zinth, H. Dube, *J. Phys. Chem. Lett.* **2017**, *8*, 1585–1592; f) F. F. Graupner, T. T. Herzog, F. Rott, S. Oesterling, R. de Vivie-Riedle, T. Cordes, W. Zinth, *Chem. Phys.* **2018**, *515*, 614–621; g) J. Wang, K. Rück-Braun, *ChemPhotoChem* **2017**, *1*, 493–498; h) Y. Liu, J. Luo, *J. Photochem. Photobiol. A* **2019**, *371*, 336–340; i) M. R. Lea, V. G. Stavros, R. J. Maurer, *ChemPhotoChem* **2022**, *6*, e202100290.

[14] a) M. Guentner, M. Schildhauer, S. Thumser, P. Mayer, D. Stephenson, P. J. Mayer, H. Dube, *Nat. Commun.* **2015**, *6*, 8406; b) A. Gerwien, P. Mayer, H. Dube, *J. Am. Chem. Soc.* **2018**, *140*, 16442–16445; c) E. Uhl, S. Thumser, P. Mayer, H. Dube, *Angew. Chem. Int. Ed.* **2018**, *57*, 11064–11068; *Angew. Chem.* **2018**, *130*, 11231–11235; d) A. Gerwien, P. Mayer, H. Dube, *Nat. Commun.* **2019**, *10*, 4449; e) E. Uhl, P. Mayer, H. Dube, *Angew. Chem. Int. Ed.* **2020**, *59*, 5730–5737; *Angew. Chem.* **2020**, *132*, 5779–5786; f) N. N. Bach, V. Josef, H. Maid,

Angew. Chem. Int. Ed. **2022**, *61*, e202210855 (7 of 8)

© 2022 The Authors. Angewandte Chemie International Edition published by Wiley-VCH GmbH

H. Dube, *Angew. Chem. Int. Ed.* **2022**, *61*, e202201882; *Angew. Chem.* **2022**, *134*, e202201882; g) A. Gerwien, F. Gnannt, P. Mayer, H. Dube, *Nat. Chem.* **2022**, *14*, 670–676.

[15] a) S. Wiedbrauk, T. Bartelmann, S. Thumser, P. Mayer, H. Dube, *Nat. Commun.* **2018**, *9*, 1456; b) T. Bartelmann, F. Gnannt, M. Zitzmann, P. Mayer, H. Dube, *Chem. Sci.* **2021**, *12*, 3651–3659; c) K. Tanaka, K. Kohayakawa, S. Iwata, T. Irie, *J. Org. Chem.* **2008**, *73*, 3768–3774; d) H. Dube, J. Rebek Jr., *Angew. Chem. Int. Ed.* **2012**, *51*, 3207–3210; *Angew. Chem.* **2012**, *124*, 3261–3264; e) G. Moncelsi, L. Escobar, H. Dube, P. Ballester, *Chem. Asian J.* **2018**, *13*, 1632–1639; f) K. Grill, H. Dube, *J. Am. Chem. Soc.* **2020**, *142*, 19300–19307.

[16] a) T. Lougheed, V. Borisenko, T. Hennig, K. Rück-Braun, G. A. Woolley, *Org. Biomol. Chem.* **2004**, *2*, 2798–2801; b) S. Herre, T. Schadendorf, I. Ivanov, C. Herrberger, W. Steinle, K. Rück-Braun, R. Preissner, H. Kuhn, *ChemBioChem* **2006**, *7*, 1089–1095; c) T. Cordes, D. Weinrich, S. Kempa, K. Riesselmann, S. Herre, C. Hoppmann, K. Rück-Braun, W. Zinth, *Chem. Phys. Lett.* **2006**, *428*, 167–173; d) T. Cordes, C. Elsner, T. T. Herzog, C. Hoppmann, T. Schadendorf, W. Summerer, K. Rück-Braun, W. Zinth, *Chem. Phys.* **2009**, *358*, 103–110; e) S. Kitzig, M. Thilemann, T. Cordes, K. Rück-Braun, *ChemPhysChem* **2016**, *17*, 1252–1263; f) A. Sailer, F. Ermer, Y. Kraus, F. H. Lutter, C. Donau, M. Bremerich, J. Ahlfeld, O. Thorn-Seshold, *ChemBioChem* **2019**, *20*, 1305–1314; g) A. Sailer, J. C. M. Meiring, C. Heise, L. N. Pettersson, A. Akhmanova, J. Thorn-Seshold, O. Thorn-Seshold, *Angew. Chem. Int. Ed.* **2021**, *60*, 23695–23704; *Angew. Chem.* **2021**, *133*, 23888–23897.

[17] a) A. Gerwien, B. Jehle, M. Irmler, P. Mayer, H. Dube, *J. Am. Chem. Soc.* **2022**, *144*, 3029–3038; b) F. Kohl, A. Gerwien, F. Hampel, P. Mayer, H. Dube, *J. Am. Chem. Soc.* **2022**, *144*, 2847–2852.

[18] D. Hean, L. G. Alde, M. O. Wolf, *J. Mater. Chem. C* **2021**, *9*, 6789–6795.

[19] F. Kink, M. P. Collado, S. Wiedbrauk, P. Mayer, H. Dube, *Chem. Eur. J.* **2017**, *23*, 6237–6243.

[20] T. Cordes, T. Schadendorf, B. Priewisch, K. Rück-Braun, W. Zinth, *J. Phys. Chem. A* **2008**, *112*, 581–588.

[21] J. E. Zweig, T. R. Newhouse, *J. Am. Chem. Soc.* **2017**, *139*, 10956–10959.

[22] a) T. Arai, M. Ikegami, *Chem. Lett.* **1999**, *28*, 965–966; b) M. Ikegami, T. Suzuki, Y. Kaneko, T. Arai, *Mol. Cryst. Liq. Cryst. Sci. Technol. Sect. A* **2000**, *345*, 113–118.

[23] a) S. Crespi, N. A. Simeth, B. König, *Nat. Chem. Rev.* **2019**, *3*, 133–146; b) J. Calbo, C. E. Weston, A. J. White, H. S. Rzepa, J. Contreras-Garcia, M. J. Fuchter, *J. Am. Chem. Soc.* **2017**, *139*, 1261–1274.

[24] M. Irie, in *Organic photochromic and thermochromic compounds*, Springer, Berlin, **2002**, pp. 207–222.

[25] L. Vogel, P. Wonner, S. M. Huber, *Angew. Chem. Int. Ed.* **2019**, *58*, 1880–1891; *Angew. Chem.* **2019**, *131*, 1896–1907.

[26] J. E. Zweig, T. A. Ko, J. Huang, T. R. Newhouse, *Tetrahedron* **2019**, *75*, 130466.

[27] J. P. J. Bruekers, R. Bakker, P. B. White, P. Tinnemans, J. A. A. W. Elemans, R. J. M. Nolte, *Tetrahedron* **2021**, *102*, 132499.

[28] Deposition numbers 2177529 (for Het-HTI *Z*-**1**), 2192395 (for Het-HTI *Z*-**4**), 2177530 (for Het-HTI *E*-**8**) and 2177531 (for Het-HTI *Z*-**10**) contain the supplementary crystallographic data for this paper. These data are provided free of charge by the joint Cambridge Crystallographic Data Centre and Fachinformationszentrum Karlsruhe Access Structures service.

[29] P. Lentes, E. Stadler, F. Rohricht, A. Brahms, J. Grobner, F. D. Sonnichsen, G. Gescheidt, R. Herges, *J. Am. Chem. Soc.* **2019**, *141*, 13592–13600.

[30] G. A. Schick, T. M. Cooper, R. A. Holloway, L. P. Murray, R. R. Birge, *Biochemistry* **1987**, *26*, 2556–2562.

[31] a) E. A. Hill, M. L. Gross, M. Stasiewicz, M. Manion, *J. Am. Chem. Soc.* **1969**, *91*, 7381–7392; b) C. Hansch, A. Leo, D. Hoekman, in *ACS Professional Reference Book, Vol. 2* (Eds.: C. Hansch, A. Leo, D. H. Hoekman), American Chemical Society, Washington, DC, **1995**.